

# Comparison of 4.5 kV SiC JBS and Si PiN Diodes for 4.5 kV Si IGBT Anti-parallel Diode Applications<sup>†</sup>

Tam Duong<sup>1</sup>, Allen Hefner<sup>1</sup>, Karl Hobart<sup>2</sup>, Sei-Hyung Ryu<sup>3</sup>, David Grider<sup>3</sup>, David Berning<sup>1</sup>, Jose M. Ortiz-Rodriguez<sup>1</sup>, Eugene Imhoff<sup>2</sup>, Jerry Sherbondy<sup>4</sup>

<sup>1</sup>National Institute of Standards and Technology, Gaithersburg, MD 20899

<sup>2</sup>Naval Research Laboratory, Washington, D.C. 20375

<sup>3</sup>Cree Inc., Durham, NC 27703

<sup>4</sup>Powerex, Inc., Youngwood, PA 15697

**Abstract**—A new 60 A, 4.5 kV SiC JBS diode is presented, and its performance is compared to a Si PiN diode used as the anti-parallel diode for 4.5 kV Si IGBTs. The I-V, C-V, reverse recovery, and reverse leakage characteristics of both diode types are measured. The devices are also characterized as the anti-parallel diode for a 4.5 kV Si IGBT using a recently developed high-voltage, double-pulse switching test system. The results indicate that SiC JBS diodes reduce IGBT turn-on switching losses by about a factor of three in practical applications. Furthermore, the peak IGBT current at turn-on is typically reduced by a factor of six, resulting in substantially lower IGBT stress. Circuit simulator models for the 4.5 kV SiC JBS and Si PiN diodes are also developed and compared with measurements.

**Keywords:** Silicon carbide (SiC); medium-voltage; high-frequency; Junction Barrier Schottky (JBS); hybrid half-bridge module; power systems.

## I. INTRODUCTION

Silicon carbide (SiC) Junction Barrier Schottky (JBS) rectifiers have advantages compared to silicon (Si) PiN diodes for switching applications due to the superior properties of SiC material such as higher breakdown electric field ( $2 \times 10^6$  V/cm to  $4 \times 10^6$  V/cm) and higher temperature capability [1]. Today, SiC JBS diodes have established widespread commercial acceptance in the low-voltage range (600 V to 1700 V) with a market penetration that is growing exponentially. High-voltage (10 kV) SiC JBS diodes have also recently been demonstrated as the anti-parallel diode for SiC metal-oxide-semiconductor field-effect transistors (MOSFETs) in 10 kV, 100 A half-bridge modules, and these modules are being applied to demonstrate a 13.8 kV,

2.75 MVA Solid State Power Substation [2]. Although the 10 kV SiC devices represent a transformational technology, it is expected to take some time before such products appear on the market, largely due to the relative lack of maturity of the SiC MOSFETs. However, medium-voltage SiC JBS diodes could be employed sooner as they can be used as the anti-parallel diodes for medium-voltage Si Insulated Gate Bipolar Transistors (IGBTs) that have already been established in the marketplace [3].

The purpose of this paper is to present a detailed comparison of 4.5 kV SiC JBS and Si PiN [4] diodes and to evaluate the benefits of SiC JBS diodes when they are used as the anti-parallel diodes for 4.5 kV Si IGBTs. This paper also presents the 4.5 kV SiC JBS diode development and develops models for the SiC JBS and Si PiN diodes. These models are being used with a 4.5 kV Si IGBT model to optimize the design of high current hybrid Si-IGBT/SiC-JBS modules. The models are based on previously developed Si IGBT [5] and SiC JBS and SiC PiN diode [6] models where the corresponding automated model parameter extraction tools [7, 8] are used to determine the model parameters of the devices from measured data.

The measured results show that the 4.5 kV SiC JBS diodes have reverse recovery switching performance that is far superior to that of 4.5 kV Si PiN diodes. When they are used as anti-parallel diodes for 4.5 kV IGBTs, a substantial improvement in both the diode and IGBT losses is achieved. Furthermore, reduced current spike stress on the IGBT and module package is observed. Lower levels of electromagnetic interference can be expected because the peak switching current is reduced and because JBS diodes do exhibit the snappy recovery that may occur with PiN diodes.

<sup>†</sup> Contribution of NIST, not subject to copyright. The devices discussed in this paper were provided by NRL. NIST does not recommend or endorse the devices as the best available for the purpose.

## II. MEDIUM-VOLTAGE SiC JBS DIODE DEVELOPMENT

Medium-voltage (4.5 V to 6.5 kV) IGBT modules have many applications ranging from medium-voltage and high-power motor drives to high voltage direct current (HVDC) and flexible AC transmission systems (FACTS) converters. The anti-parallel diodes in these modules are the major limiting factor in performance due to losses and current stress that result from the poor diode reverse recovery characteristics. This has become a critical problem for naval applications which require medium voltage power systems to be built on relatively small platforms due to the large increase in electrical power demanded, by e.g., hybrid- or all-electric propulsion, high power radar, and new weapons systems. The 4.5 kV SiC JBS diodes and the 4.5 kV Si-IGBT/SiC-JBS hybrid modules being developed in this work are motivated by this critical need. It is expected that the use of these hybrid modules for the naval platform will enable reduced size, weight, and cooling requirements and will result in improved operational capabilities and significant fuel savings.

Fig. 1 shows a schematic cross-section of the 4.5 kV 4H-SiC JBS diode developed in this work. The n- epitaxial layer of the diodes is  $\sim 50 \mu\text{m}$  thick, doped at  $\sim 1 \times 10^{15} \text{ cm}^{-3}$  and was grown on 100 mm diameter 4H-SiC substrates that had a bulk resistivity of  $0.02 \Omega\cdot\text{cm}$  and that were cut  $4^\circ$  off of the [0001] axis. During fabrication, aluminum was first implanted in a gridded pattern across the active area of the devices to provide the p-n junction barrier of the JBS diode. The diodes were terminated with a boron-implanted junction termination extension (JTE). Following implant activation at  $1650^\circ\text{C}$ , the surface of the diodes was passivated with  $\text{SiO}_2$ , and a backside ohmic contact was deposited and annealed. Windows were then opened over the diodes, into which the Ni Schottky metal and subsequently an Al overlayer were deposited. These windows define the active area for forward conduction which is  $0.456 \text{ cm}^2$ .

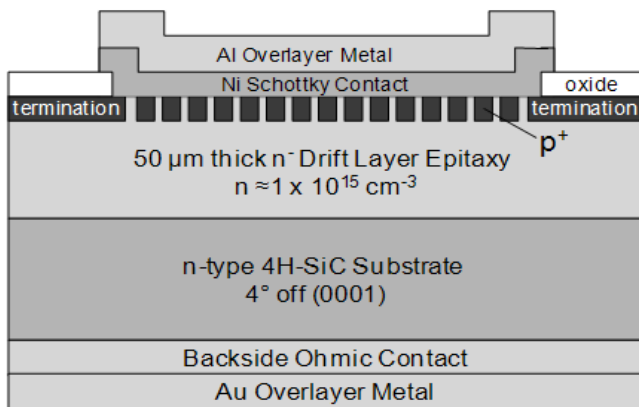


Fig. 1: Schematic cross-section through the 4.5 kV 4H-SiC JBS diode.

Finally, a thick Au layer was deposited on the wafer backside for die attach purposes. The overall chip size is  $(8 \times 8) \text{ mm}^2$ . The devices were designed for a current density of approximately  $30 \text{ A/cm}^2$ . To realize the 60 A JBS

diode, four 15 A diodes were paralleled in a discrete Powerex package rated for 4.5 kV.

Fig. 2 shows the measured temperature dependence of the 4.5 kV, 60 A SiC JBS diode reverse recovery characteristics compared with those of the 4.5 kV, 60 A Si PiN diode that is used in commercial 4.5 kV IGBT modules. These waveforms were obtained using the double-pulse switching system described below with an IGBT gate resistor of  $100 \Omega$ , diode forward current of 40 A, and a bus voltage of 3 kV. As shown in Fig. 2, the peak reverse recovery current and the total recovered charge, which is determined by the diode junction capacitance, for the SiC JBS diode remains unchanged with temperature. By contrast, the peak reverse recovery current for the Si PiN diode, which is determined by minority carrier charge decay time, increases with temperature. Compared to the Si PiN, the SiC JBS diode reduces the peak reverse recovery current by more than a factor of six and reduces the total reverse recovery charge (area below zero current) from  $66 \mu\text{C}$  to  $2.5 \mu\text{C}$ . Thus, the SiC JBS diode enables a much higher switching frequency and lower loss with reduced current spike stress on the die, package, and system.

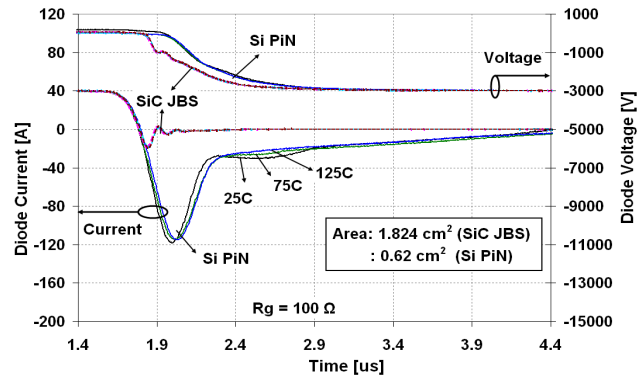


Fig. 2: Measured diode reverse recovery temperature-dependence of the 4.5 kV, 60 A Si PiN and SiC JBS with IGBT gate resistor of  $100 \Omega$ .

## III. CHARACTERIZATION OF 4.5 KV Si PiN AND SiC JBS DIODES

The measured and simulated diode current-voltage, capacitance-voltage, and reverse recovery characteristics versus temperature are given in Figs. 3-8 for both the 4.5 kV, 60 A Si PiN diode and the 4.5 kV, 60 A SiC JBS diode. The leakage current versus temperature is shown in Fig. 9.

Figs. 3 and 4 show the I-V characteristics of the 4.5 kV, 60 A SiC JBS and Si PiN diodes at three different temperatures of  $25^\circ\text{C}$ ,  $75^\circ\text{C}$ , and  $125^\circ\text{C}$ , respectively. The results indicate that the SiC JBS diode begins to conduct at approximately 1.2 V as determined by the Schottky barrier height, versus 0.6 V for the Si PiN diode as determined by the built-in potential of the P-i-N junction. The results also indicate that both devices have similar performance; however the SiC JBS has a positive temperature coefficient resulting in a better current sharing for paralleled SiC diodes.

Figs. 5 and 6 show the capacitance-voltage characteristics for 4.5 kV, 60 A SiC JBS and Si PiN diodes at 25 °C, respectively. These measurements were made using a new test system that safely and accurately allows the capacitance voltage (C-V) measurements up to 5 kV [9]. The results indicate that the junction capacitance of the SiC JBS diode is approximately eight times larger than that same current-rated Si PiN diode. Although the capacitance is larger, it still produces far less reverse recovery charge than the Si PiN, as shown below, and the capacitance is better

behaved in that there is no possibility of an abrupt (snappy) change in capacitance as there is with the PiN diode under certain conditions.

Figs. 7 and 8 show the reverse recovery characteristics for the 4.5 kV, 60 A SiC JBS and Si PiN diodes with the forward current of 30 A, switching voltage of 2.25 kV at three different values of reverse di/dt (40 A/μs, 80 A/μs, and 170 A/μs) at 25 °C, and with a low external driver capacitance. These measurements were obtained using a

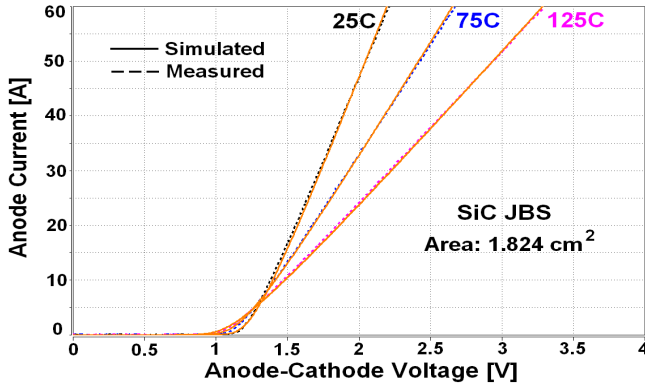


Fig. 3: Measured (dashed) and simulated (solid) forward characteristics for a 4.5 kV, 60 A SiC JBS diode.

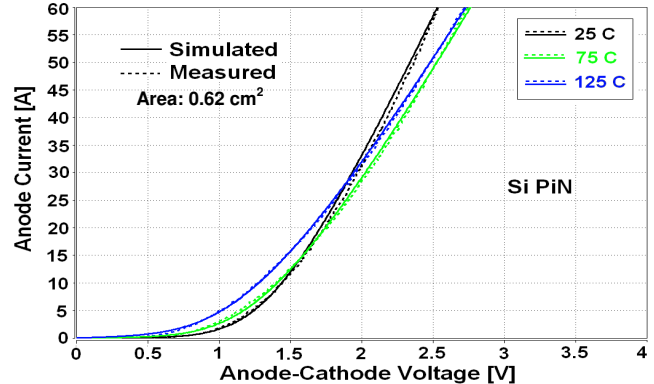


Fig. 4: Measured (dashed) and simulated (solid) forward characteristics for a 4.5 kV, 60 A Si PiN diode.

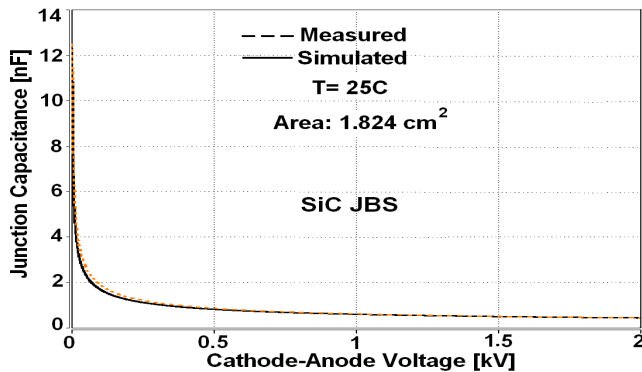


Fig. 5: Measured (dashed) and simulated (solid) junction capacitance for a 4.5 kV, 60 A SiC JBS diode at 25 °C.

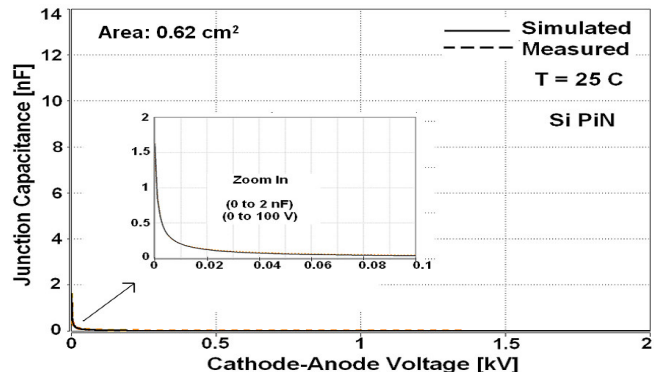


Fig. 6: Measured (dashed) and simulated (solid) junction capacitance for a 4.5 kV, 60 A Si PiN diode at 25 °C.

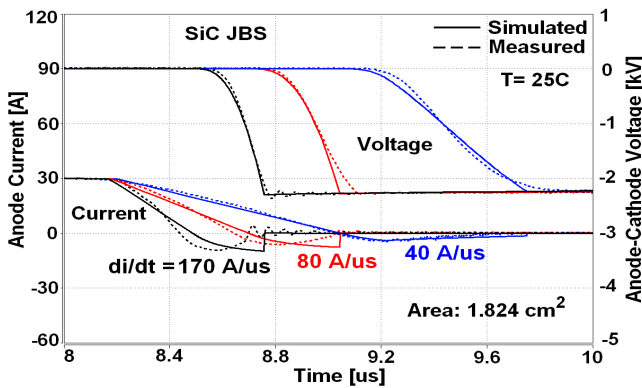


Fig. 7: Measured (dashed) and simulated (solid) reverse recovery at different di/dt for a 4.5 kV, 60 A SiC JBS diode at 25 °C.

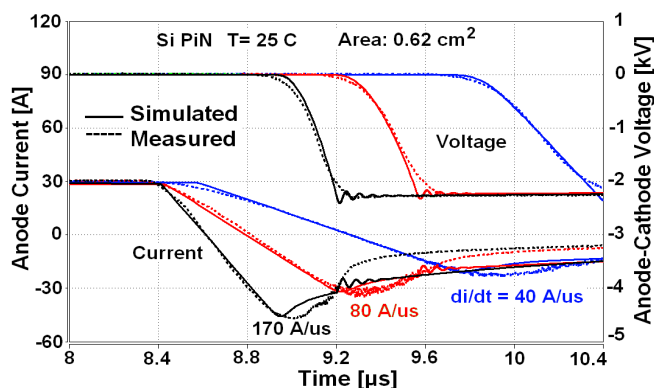


Fig. 8: Measured (dashed) and simulated (solid) reverse recovery at different di/dt for a 4.5 kV, 60 A Si PiN diode at 25 °C.

custom 18-vacuum-tube high-voltage reverse recovery test system [6] that allows independent control of  $di/dt$  via tube driver and also  $dv/dt$  via an external driver capacitance that can be applied across the device under test (DUT); this is required to develop and validate models that are applicable for the full range of circuit conditions. The results indicate that, compared to the Si PiN diode, the SiC JBS diode reduces the peak reverse recovery current by more than a factor of 5, and reduces the reverse recovery charge by more than a factor of 20.

Fig. 9 shows the measured reverse leakage characteristics for a 4.5 kV, 60 A SiC JBS diode (dashed) and a 4.5 kV, 60 A Si PiN diode (solid) at 25 °C, 50 °C, 75 °C, 100 °C, and 125 °C. The results indicate that, compared to the Si PiN diode, the SiC JBS diode has lower leakage current for anode voltage levels below 4 kV for all temperatures and that its leakage has less variation with temperature but more variation with voltage.

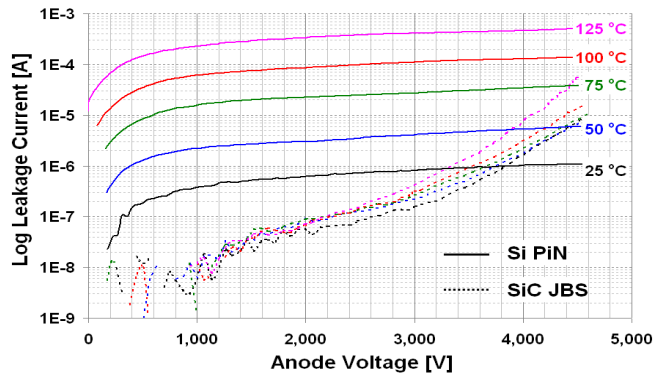


Fig. 9: Anode leakage for the 4.5 kV, 60 A SiC JBS diode (dashed) and Si PiN diode (solid) at 25 °C, 50 °C, 75 °C, 100 °C, and 125 °C.

#### IV. INTERACTION OF 4.5 kV Si IGBT SWITCH WITH 4.5 kV Si PiN AND SiC JBS DIODES

Figs. 10 and 11 depict the double-pulse switching test circuit and timing waveforms that are used to measure the circuit interaction between the Si IGBT and the SiC JBS and SiC PiN diodes [10] using the gate driver of [11]. Note that this circuit can emulate a half-bridge module where the IGBT anti-parallel diode of the high-side switch is recovered by the low-side switch, or this circuit can also represent a single switch and commutating diode in a boost converter. This system enables flexible control of the current, temperature, bus voltage, drive circuit, and load circuit. Figs. 12-15 show IGBT and diode current and voltage waveforms during the IGBT turn-on (a) when the diode undergoes reverse recovery, and turn-off (b) for both the SiC JBS and Si PiN diodes at different switching currents and different IGBT gate resistors.

Fig. 12 shows the measured inductive load turn-on (a) and turn-off (b) waveforms of the 4.5 kV, 60 A Si IGBT for different gate resistors (i.e., 51 Ω and 100 Ω), a switching current of 40 A, a collector-emitter voltage of 3 kV, and IGBT and diode temperatures of 25 °C, where the dashed

waveforms are for the SiC JBS and the solid waveforms are for the Si PiN. Note that the trigger point in Fig. 12 (a) was chosen for easy comparison of reverse recovery peaks, so the waveforms do not demonstrate the delay that results for larger gate resistance.

Fig. 13 shows the measured inductive load turn-on (a) and turn-off (b) waveforms of the 4.5 kV, 60 A Si IGBT for different switching current (i.e., 10 A, 20 A, 30 A, and 40 A), a gate resistor of 100 Ω, a collector-emitter voltage of 3 kV, and IGBT and diode temperatures of 25 °C, where the dashed waveforms are for the SiC JBS and the solid waveforms are for the Si PiN.

Fig. 14 shows the measured diodes waveforms (dashed waveforms are for the SiC JBS and solid waveforms are for the Si PiN) for the same conditions and trigger points as Fig. 12 (a). The results indicate that the IGBT experiences extreme current spike stress from the Si PiN that can only be minimized by increasing the gate resistance which adds additional loss and results in switching delay, whereas the device can be switched much faster with the SiC JBS diode.

Fig. 15 shows the measured diode reverse recovery for the inductive load turn-on of the 4.5 kV, 60 A Si IGBT for different switching currents with a gate resistance of 100 Ω, collector-emitter voltage of 3 kV, and IGBT and diode temperatures of 25 °C, where the dashed waveforms are for the SiC JBS and the solid waveforms are for the Si PiN. The waveforms of Fig. 2 were obtained similarly to those of Figs. 14 and 15. The combined results indicate that the reverse recovery current increases with temperature and switching current for the Si PiN, but remains constant for the SiC JBS.

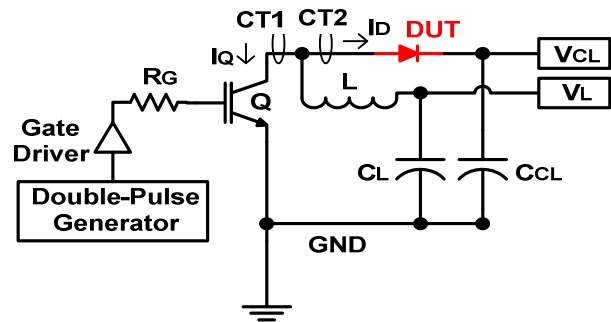


Fig. 10: Circuit configuration for characterizing diode reverse recovery.

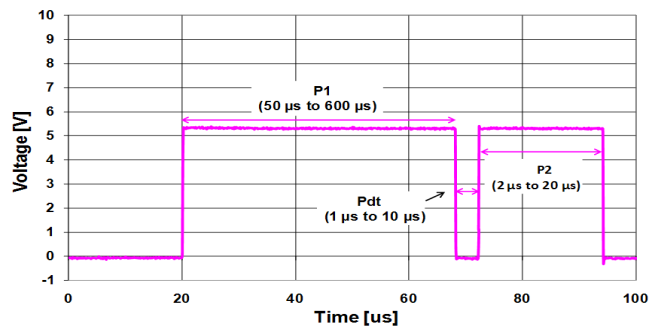
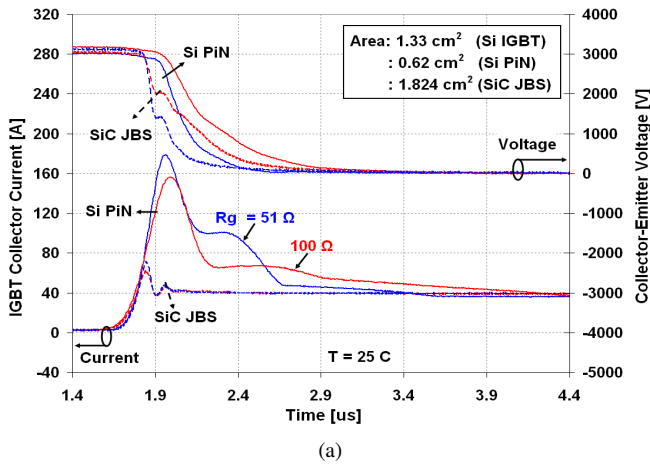
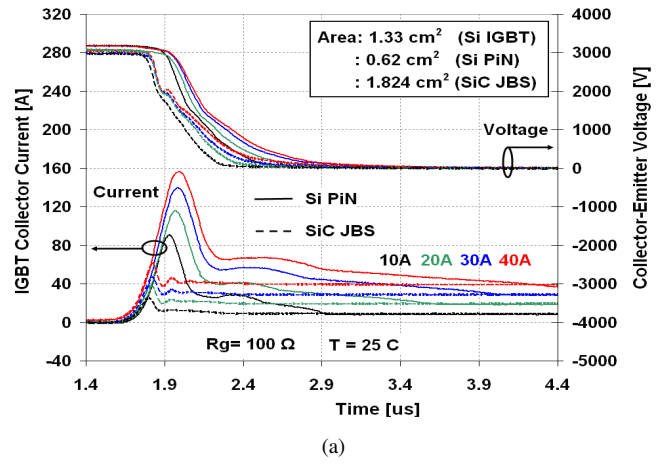


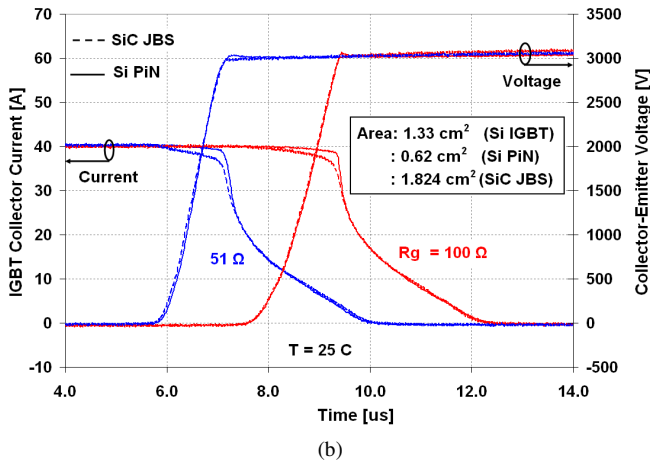
Fig. 11: The output waveforms of the double-pulse generator.



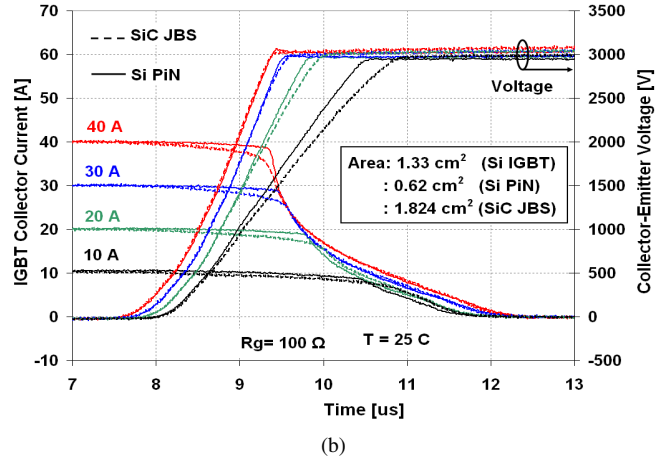
(a)



(a)



(b)



(b)

**Fig. 12:** Gate resistor dependence of 4.5 kV, 60 A Si IGBT inductive load turn-on (a) and turn-off (b) with a 4.5 kV, 60 A SiC JBS diode (dashed) and a 4.5 kV, 60 A Si PiN diode (solid).

**Fig. 13:** Current dependance of inductive-load turn-on (a) and turn-off (b) switching waveforms for the Si IGBT with the SiC JBS diode (dashed) and the Si PiN diode (solid).

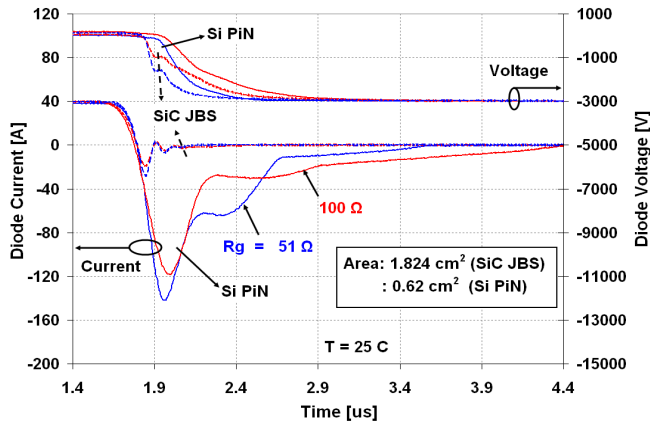


**Fig. 14:** Reverse recovery waveforms of a 4.5 kV, 60 A SiC JBS diode (dashed) and a 4.5 kV, 60 A Si PiN diode (solid) for the same conditions as Fig.12 (a).

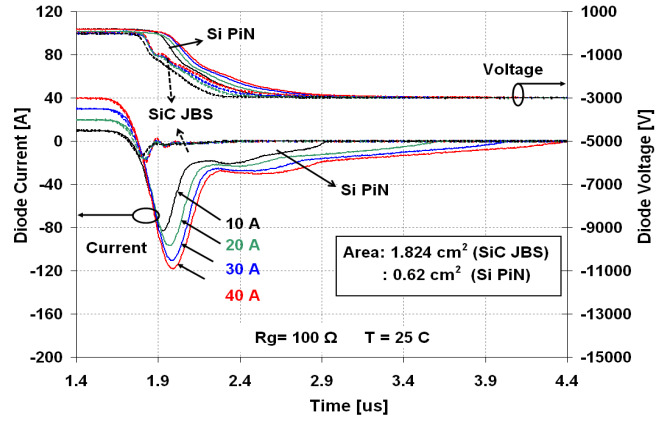
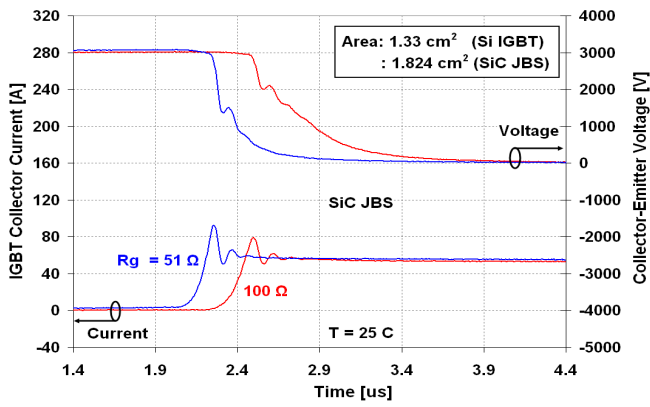


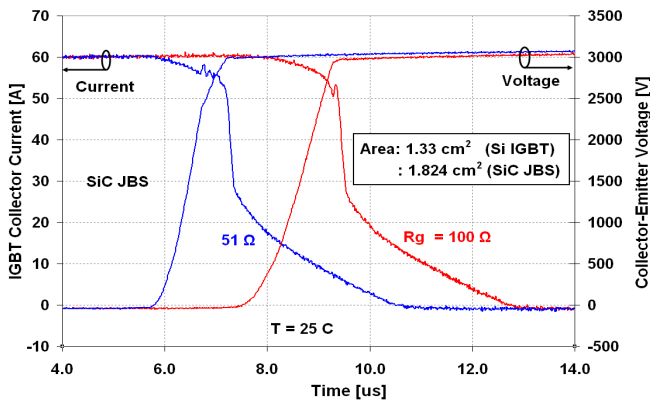
**Fig. 15:** Reverse recovery waveforms of a 4.5 kV, 60 A SiC JBS diode (dashed) and a 4.5 kV, 60 A Si PiN diode (solid) for the same conditions as Fig. 13 (a).

To demonstrate the full capability of the SiC JBS diodes, Fig. 16 shows the measured inductive load turn-on (a) and turn-off (b) waveforms of the 4.5 kV, 60 A Si IGBT for different gate resistors, a switching current of 60 A, a collector-emitter voltage of 3 kV, and IGBT and diode

temperatures of 25 °C. Note that the measurements of Fig. 16 were performed only for the SiC JBS diode, because the high reverse recovery current of the Si PiN for the gate resistors used and a 60 A switching current has a high probability of failing either the IGBT or the diode .



(a)



(b)

Fig. 16: Gate resistor dependence of the Si IGBT inductive load turn-on (a) and turn-off (b) with the SiC JBS diode.

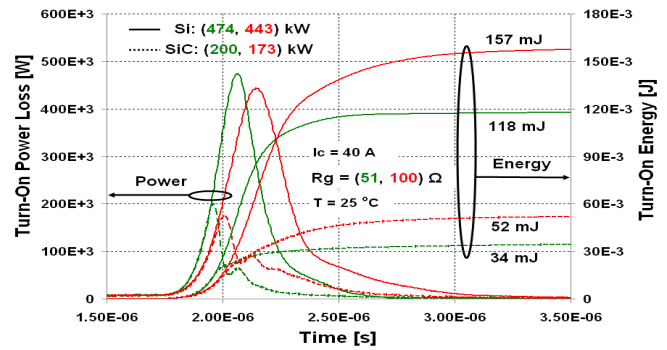
## V. SWITCHING LOSS CALCULATIONS

Table 1 summarizes the calculated switching loss in the Si IGBT for the various switching currents and gate resistors studied and when both the Si-PiN and SiC-JBS diodes are used. The results are obtained using the measured data from the circuit shown in Fig. 10. It is clear that for all conditions both the peak IGBT power dissipation during turn on and the total IGBT switching energy are lower when the SiC-JBS diode is used rather than the Si-PiN diode.

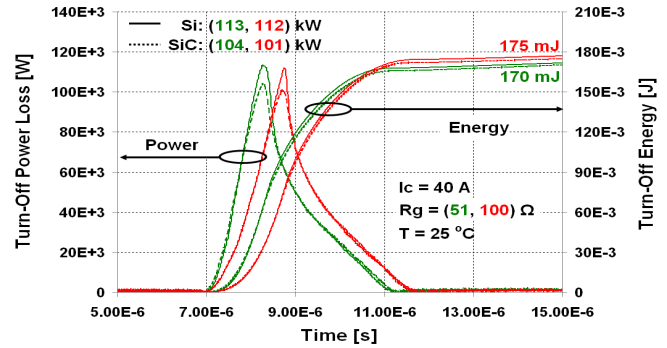
Fig. 17 shows an example of how the turn-on (a) and turn-off (b) IGBT switching losses are calculated for the SiC JBS diode (dashed) and the Si PiN diode (solid), where two different gate resistors (i.e., 51 Ω (in green) and 100 Ω (in red)) are indicated and the collector-emitter voltage is 3 kV, the switching current is 40 A, and the IGBT and diode temperature are 25 °C. As another example, Fig. 18 shows turn-on (a) and turn-off (b) power and switching energy representing the data as the 60 A shown in Fig. 16.

## VI. CONCLUSIONS

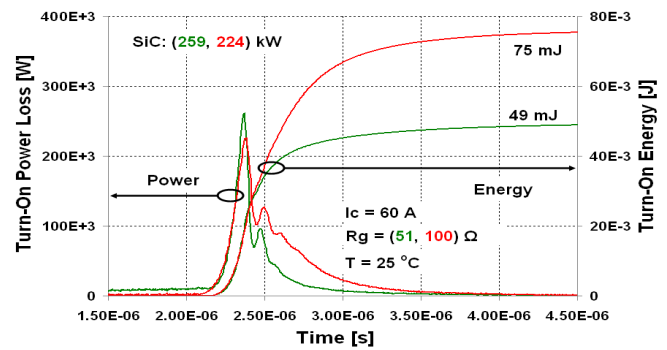
This paper presents a new 4.5 kV SiC JBS diode, gives detailed measured and simulated comparisons between medium-voltage SiC JBS and Si PiN diodes, and evaluates



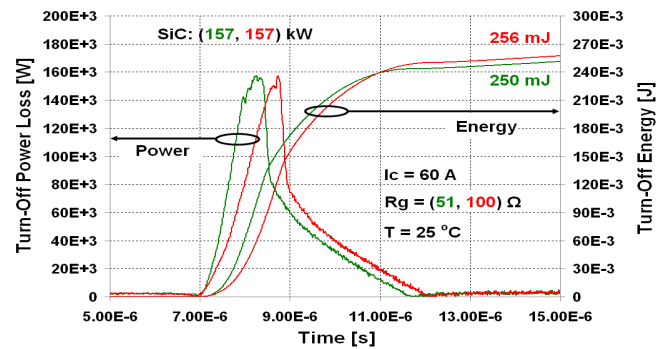
(a)



(b)



(a)



(b)

Fig. 18: Turn-on (a) and turn-off (b) power and energy waveforms for the Si IGBT inductive-load switching with the SiC JBS diode at 60 A.

the benefits of SiC JBS diodes when used as the anti-parallel diode for 4.5 kV Si IGBTs. The results show that the use of the SiC JBS diode in place of the Si PiN diode results in about a factor of 3 reduction in turn-on switching loss in the Si IGBT due to the reverse recovery of the Si PiN diode. This reduction in switching loss comes from the SiC JBS diode having better than a factor of 6 reduction in peak diode reverse recovery current and better than a factor of 20 reduction in reverse recovered charge compared to the Si PiN diode. Furthermore, the reverse recovery loss within the SiC JBS diodes themselves are virtually zero since the reverse recovery current is due to charging a junction capacitance, whereas the reverse recovery loss in the Si PiN represents another significant loss and heating mechanism. This work demonstrates that medium-voltage SiC JBS diodes provide breakthrough performance and have tremendous benefits when used as the anti-parallel or commutation diode for medium-voltage Si IGBTs.

### REFERENCES

- [1] A. R. Hefner, R. Singh, J. Lai, D. W. Berning, S. Bouche, C. Chapuy, "SiC Power Diodes Provide Breakthrough Performance for a Wide Range of Applications," IEEE Transactions on Power Electronics, vol. 16, no. 2, March 2001, pp. 273-280.
- [2] A. Hefner, "Performance Analysis of 10 kV, 100 A SiC Half-Bridge Power Modules," Proceedings of the Government Microcircuit Applications and Critical Technology Conference (GOMACTech) 2008, March 17-20, 2008, Las Vegas, NV, pp. 361-364.
- [3] Silicon IGBT: <http://www.pwr.com/pwr/docs/qis4506001.pdf>.
- [4] Si PiN diodes: <http://www.pwr.com/pwr/docs/qrs4506001.pdf>.
- [5] A. R. Hefner, Jr., "A Dynamic Electro-Thermal Model for the IGBT," in the IEEE Trans. on Industry Applications, vol. 30, no. 2, pp. 394-405, 1994.
- [6] T. R. McNutt, A. Hefner, Jr., H. Mantooth, J. Duliere, D. Berning, R. Singh, "Silicon Carbide PiN and Merged PiN Schottky Power Diode Models Implemented in the Saber Circuit Simulator," IEEE Trans. Power Electron., vol. 19, no. 3, pp. 573-581, 2004.
- [7] N. Yang, T. Duong, J.-O. Jeong, A. Hefner, K. Meehan, "Automated Parameter Extraction Software for Silicon and High-Voltage Silicon Carbide Power Diodes," in the IEEE COMPEL 2010, at the University of Colorado, Boulder, Colorado, June 28-30, 2010.
- [8] T. R. McNutt, A. R. Hefner, H. A. Mantooth, J. L. Duliere, D. W. Berning, R. Singh, "Parameter Extraction Sequence for Silicon Carbide Schottky, Merged PiN Schottky, and PiN Power Diode Models," IEEE, 2002, pp. 1269-1276.
- [9] P. Ralston, T. Duong, N. Yang, D. Berning, C. Hood, A. Hefner, K. Meehan, "High-Voltage Capacitance Measurement System for SiC Power MOSFETs," in Energy Conversion Congress and Exposition, 2009. ECCE, pp. 1472-1479.
- [10] D. Berning, A. Hefner, J. M. Ortiz-Rodriguez, C. Hood, A. Rivera, "Generalized Test Bed for High-Voltage, High-Power SiC Device Characterization," Proceedings of the 2006 IEEE Industry Applications Society (IAS) Annual Meeting, October 08-12, 2006, Tampa, FL, pp. 338-345.
- [11] D. W. Berning, T. H. Duong, J. M. Ortiz-Rodriguez, A. Rivera-Lopez, A. R. Hefner Jr., "High-Voltage Isolated Gate Drive Circuit for 10 kV, 100 A SiC MOSFET/JBS Power Modules," Proceedings of the 43th Annual Meeting of the IEEE Industry Applications Society (IAS 2008), October 5-9, 2008, in Edmonton, Alberta, Canada.

**Table 1:** Power and Energy Calculations for 4.5 kV, 60 A Si IGBT with a 4.5 kV, 60 A, Si PiN diode or SiC JBS diode for the circuits in Fig. 10

Case #	Si IGBT with Si PiN					Si IGBT with SiC JBS Diode				
	P <sub>IGBT, ON</sub> [kW]	P <sub>IGBT, OFF</sub> [kW]	E <sub>sw, ON</sub> [mJ]	E <sub>sw, OFF</sub> [mJ]	E <sub>sw, TOTAL</sub> [mJ]	P <sub>IGBT, ON</sub> [kW]	P <sub>IGBT, OFF</sub> [kW]	E <sub>sw, ON</sub> [mJ]	E <sub>sw, OFF</sub> [mJ]	E <sub>sw, TOTAL</sub> [mJ]
1	257	25	58	46	104	68	20	12	46	58
2	315	55	86	89	175	106	48	24	89	113
3	392	82	125	131	256	127	76	34	131	165
4	443	112	157	175	332	173	101	52	175	227
5	474	113	118	170	288	200	104	34	170	204
6*	-	-	-	-	-	259	157	49	250	299
7*	-	-	-	-	-	224	157	75	256	331

Case 1: I<sub>IGBT</sub> = 10 A, V<sub>CL</sub> = 3 kV, R<sub>G</sub> = 100 Ω.

Case 2: I<sub>IGBT</sub> = 20 A, V<sub>CL</sub> = 3 kV, R<sub>G</sub> = 100 Ω.

Case 3: I<sub>IGBT</sub> = 30 A, V<sub>CL</sub> = 3 kV, R<sub>G</sub> = 100 Ω.

Case 4: I<sub>IGBT</sub> = 40 A, V<sub>CL</sub> = 3 kV, R<sub>G</sub> = 100 Ω. (See Fig. 17)

Case 5: I<sub>IGBT</sub> = 40 A, V<sub>CL</sub> = 3 kV, R<sub>G</sub> = 51 Ω. (See Fig. 17)

Case 6: I<sub>IGBT</sub> = 60 A, V<sub>CL</sub> = 3 kV, R<sub>G</sub> = 51 Ω. (See Fig. 18)

Case 7: I<sub>IGBT</sub> = 60 A, V<sub>CL</sub> = 3 kV, R<sub>G</sub> = 100 Ω. (See Fig. 18)

\*Note: The measurements for cases 6 and 7 were not performed using the Si PiN.